



RESEARCH ARTICLE

The role of weak C–H···O hydrogen bond in alcohol–water mixtures

Tao Li¹ | Wei Fan² | Jin Sun¹ | Yuanqin Yu¹  | Xiaoguo Zhou²  |
Chuanmei Xie¹ | Shilin Liu²¹Department of Physics, Anhui University, Hefei, China²Hefei National Laboratory for Physical Sciences at the Microscale, iChEM (Collaborative Innovation Center of Chemistry for Energy Materials), Department of Chemical Physics, University of Science and Technology of China, Hefei, China**Correspondence**

Yuanqin Yu, Department of Physics, Anhui University, Hefei, Anhui, 230601, China.

Email: yyq@ahu.edu.cn

Shilin Liu, Hefei National Laboratory for Physical Sciences at the Microscale, iChEM (Collaborative Innovation Center of Chemistry for Energy Materials), Department of Chemical Physics, University of Science and Technology of China, Hefei 230026, China.

Email: sliu@ustc.edu.cn**Funding information**

National Natural Science Foundation of China, Grant/Award Numbers: 21873002, 21773001, 21727804, 21873089, 22073088

Abstract

Does the weak C–H···O hydrogen bonding interaction coexist in liquid when it competes with conventional hydrogen bonding interaction? The Raman spectroscopic studies were performed for deuterated 2-propanol/water (CD₃CHOHCD₃) mixture in the C–H stretching region as a function of concentration and temperature. Combined with theoretical calculations, it is shown that both conventional O–H···O hydrogen bond and weak C–H···O hydrogen bond coexist in 2-propanol/water solution and should be responsible for the observed C–H blue shift in concentration-dependent spectra. At relatively high alcohol concentrations, the O–H···O hydrogen bond plays a dominant role, whereas with the increase of water concentrations, the cooperative effect between C–H···O and O–H···O hydrogen bonds play a more significant role, responsible for continuously increased C–H blue shift. Furthermore, the opposite temperature dependence was observed for the C–H stretching spectra of 2-propanol/water and methanol–water mixtures, which were explained as a result of the competition and balance between O–H···O and C–H···O hydrogen bonds at high temperature. The results not only show the role of secondary hydrogen bonds in the hydrated process of amphiphilic molecules but also demonstrate that the temperature can be used as a means of triggering and investigating weak C–H···O interaction in liquid.

KEYWORDS

alcohol–water mixture, blue shift, cooperative effect, temperature, weak hydrogen bond

1 | INTRODUCTION

Hydrogen bond (H-bond) has been discovered for more than a hundred years as a topic of lasting interest due to its significance in many fields such as physics, chemistry, biology, and life science.^[1,2] The H-bonding interactions, which are formed by a C–H group acting as a proton donor to O atom, represent one of the most common H-bonds in molecular processes. Although carbon is not particularly electronegative, it has been suggested that

the C–H···O H-bond plays an important role in solvation,^[3–5] molecular self-assembly,^[6] molecular recognition,^[7] structural stability,^[8–12] stereoselective reactions,^[13,14] and protein–protein interaction.^[15,16] For example, the C–H···O H-bond has been demonstrated as a determinant of stability and specificity in transmembrane helix interactions.^[8]

Generally, a characteristic feature of the formation of the conventional X–H···Y H-bonds is X–H bond lengthening with a concomitant red shift of the X–H stretching

wavenumber and increased intensity in their infrared spectra, where X and Y are electronegative atoms such as O and F. However, the formation of C–H...O H-bond leads to blue shift of C–H stretching wavenumber with a shortening of the C–H bond. Owing to this unconventional behavior, the C–H...O H-bond is also called as improper blue-shifted H-bond. A number of theoretical attention has been devoted to explain the nature of C–H...O H-bond,^[17–19] but a unified view is still lacking.

Compared to conventional H-bond, another feature of C–H...O is weakness, and thus, direct experimental evidence for its existence is very difficult to be obtained. Very recently, using linear and non-linear IR spectroscopy, Kankanamge et al. proved the presence of the elusive C–H...O H-bond formed between the chloroform C–H group and an amide carbonyl oxygen in liquid solution at room temperature.^[4] In a recent study, the formation of C–H...O in solid has also been shown using atomic force microscopy.^[20] Due to the weakness, the spectroscopic evidence of C–H...O H-bond is easily ignored or obscured by stronger effects, especially in an aqueous system where the conventional H-bonds are usually believed to be overwhelming. In this sense, it is interesting to investigate the coexistence and competition between weak and conventional H-bonding interactions in an aqueous system.

Alcohol–water mixtures are ideal candidates for above purpose since the alcohol are typical amphiphilic molecules containing both hydrophilic and hydrophobic head groups. The mixing between alcohol and water molecules should be affected by the balance between the hydrophilic interaction and hydrophobic interaction. In addition, alcohol–water mixture exhibits many abnormal transport and thermodynamical properties such as negative excess entropy.^[21–25] These abnormal macroscopic properties should be determined by microscopic structure that are closely related to intermolecular interactions.

Various experimental techniques and theoretical methods are employed to investigate the structures of alcohol–water mixtures, including vibrational spectroscopy,^[26–28] neutron diffraction,^[29–31] nuclear magnetic resonance spectroscopy (NMR),^[32] terahertz time domain spectroscopy (THz-TDS),^[33] and X-ray absorption spectroscopy^[34–38] as well as molecular dynamical simulation (MD).^[39–41] In this work, Raman spectroscopic studies were performed on alcohol–water mixtures using the C–H stretching vibration as a probe. Compared to the O–H stretching mode, which is often used as a probe of alcohol–water mixtures, the C–H stretching vibration has two advantages. First, the C–H stretching spectra are relatively easy to be assigned, whereas the O–H stretching bands are broadened in liquid due to intermolecular interaction. Although the C–H

stretching spectrum also suffers spectral overlapping from the interferences of different C–H groups, the isotope substitution can help to solve it. Second, the C–H stretching vibration offers a direct detection of weak C–H...O interaction since it is more sensitive to the hydrated environment around C–H group.

Among water-soluble monohydric alcohols, 2-propanol is the simplest secondary alcohol, in which the alcohol carbon atom is simultaneously attached to two electron-donating CH₃ groups. With the increasing size of the nonpolar head group, the more pronounced effects on different thermodynamic properties can be observed. For example, while the measured excess enthalpies of mixing for methanol–water and ethanol–water mixtures were always negative for all concentrations, the excess enthalpy of mixing for 2-propanol/water mixture is only negative for concentrations of 2-propanol below 0.45.^[22] Very recently, Lam et al. measured oxygen K-edge X-ray absorption spectra of methanol/water, ethanol/water, and 2-propanol/water mixtures and suggested that the origin of negative excess entropy may be different for 2-propanol/water system and for small straight-chain alcohol–water systems such as methanol and ethanol.^[42] The formation of various hydrogen-bonded aggregates may govern the structural and dynamical change in alcohol–water mixtures. It is known that the H-bond is sensitive to external environment such as temperature and pressure. Here, we investigated the effect of concentration and temperature on Raman spectra of deuterated 2-propanol (CD₃CHOHCD₃) in the C–H stretching region with the aim to obtain more insight into the H-bonding interactions in 2-propanol/water solution, especially we pay more attention on coexistence and competition of weak and conventional H-bonds.

2 | EXPERIMENTAL AND THEORETICAL METHODS

Deuterated 2-propanol (CD₃CHOHCD₃) was purchased from ICON isotopes (99%) and used without further purification. Spectral grade methanol was purchased from Sigma-Aldrich (99.5%). The water was triply distilled. The alcohol–water solutions were prepared by volume measurement of alcohol and water to achieve the desired molar concentrations.

The instrumental parameters of Raman spectroscopy are similar to those reported previously.^[43–46] Briefly, the excitation source was 532-nm line from Coherent Verdi-5 laser with a power output of 2 W. The Raman scattering light was collected with backscattering configuration at 180° relative to the incident laser beam with a pair of $f = 2.5$ and 10-cm quartz lenses and imaged onto the

entrance slit of the monochromator (Acton Research, TriplePro) connected to a liquid-nitrogen-cooled CCD detector (Princeton Instruments, Spec-10:100B) to obtain experimental data. To obtain high spectral resolution, the 2400 groove/mm grating was used with a resolution of $\sim 1.0 \text{ cm}^{-1}$. The precision of spectral measurement was estimated to be better than 0.01 cm^{-1} from a calibration of Hg lamp. Each spectrum is an accumulation of 10 scans with a typical exposure time of 2 s. For the measurements of temperature-dependent Raman spectra, a heating bath (THD-2006, Ningbo) was used to heat the samples in a $1 \times 1\text{-cm}^2$ quartz cuvette, and the stability of temperature is controlled at 0.1°C . In order to avoid the interference from the broad O–H band shape of water, the C–H spectrum was obtained by subtracting the pure water spectrum from the solution spectrum at each concentration or temperature, both of which were measured under the same experimental conditions.

All calculations were performed with the Gaussian 16 suite of program,^[47] including optimized structures, harmonic vibrational wavenumber, and binding energies of various clusters between 2-propanol and water molecules. The hydrated clusters are generated by using the Genmer tool of the Molclus package,^[48] which has been successfully used to predict cluster geometries, and then these structures were optimized at the M06-2X/6-311++G(d,p) level. The M06-2X functional was chosen in this work because it performed well in characterizing weak intermolecular interaction in previous studies.^[49] All the calculated clusters were confirmed to be stable with no imaginary wavenumber, and a scaling factor of 0.954 was applied in order to contrast with the experiment. The binding energies of all clusters were corrected for basis set superposition error (BSSE) using the counterpoise (CP) procedure suggested by Boys and Bernardi^[50] and defined as the following:

$$\Delta E = E_{\text{cluster}} - (E_{2\text{-propanol}} + n^* E_{\text{water}}) + E_{\text{BSSE}} \quad (1)$$

where E_{cluster} , $E_{2\text{-propanol}}$, and E_{water} denote the electronic energies of hydrated clusters, alcohol monomer, and water monomer corrected by zero-point vibrational energy (ZPE), respectively.

The theory of atoms in molecules (AIM) was used to characterize the H-bonding interactions in hydrated clusters in order to obtain the information on the H-bonding critical point (HBCP), the electron density ρ and the Laplacian value of the electron density $\nabla^2 \rho$ at HBCP.^[51–53] The values of ρ and $\nabla^2 \rho$ at HBCP can be used as a criterion for hydrogen bond. According to Bader's rule, the condition of $0.002 < \rho < 0.034$ and $0.02 < \nabla^2 \rho < 0.139$ can be regarded as a true H-bond.^[52]

Generally, the larger value of ρ at HBCP, the stronger is the H-bonding interaction. The AIM calculation was carried out with the help of the Multiwfn program^[54] and visualized using VMD software (version 1.9.3).

3 | RESULTS AND DISCUSSIONS

3.1 | Concentration-dependent Raman spectra

Figure 1 displays Raman spectra of deuterated 2-propanol/water mixture in the C–H stretching region at different concentrations. To avoid spectral interference from different C–H groups, the deuterated 2-propanol ($\text{CD}_3\text{CHOHCD}_3$) was used, whose C–H stretching spectra has been well documented in previous studies.^[55] The strong band at 2887 cm^{-1} was attributed to the CH stretching vibration of methyne group of gauche conformer, whereas a very weak shoulder at about 2940 cm^{-1} was attributed to trans conformer. From Figure 1, it can be seen that the CH stretching band of $\text{CD}_3\text{CHOHCD}_3$ shifts to a higher wavenumber with the increase of water concentration. The largest blue shift at 2887 cm^{-1} is $\sim 24 \text{ cm}^{-1}$ when going from pure liquid state to aqueous solution with a molar fraction of 0.05. Similar blue shift phenomena were also observed in alcohol, pyridine and acetone aqueous solutions.^[56–58] To be contrasted, the Raman spectra of deuterated 2-propanol in CCl_4 solution are also recorded at different concentrations, as shown in Figure 2. Different from water

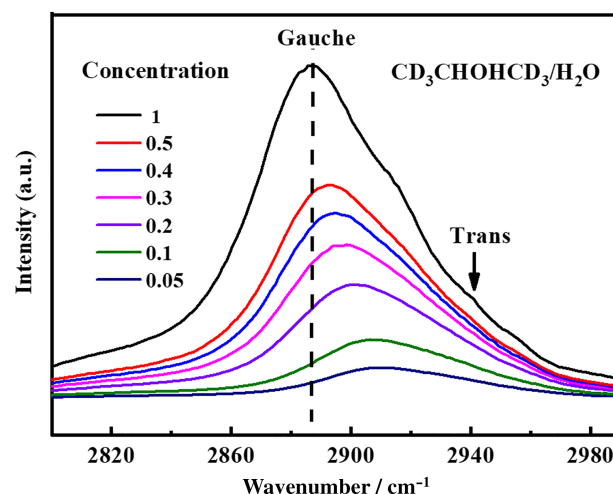


FIGURE 1 Concentration-dependent Raman spectra of deuterated 2-propanol/water ($\text{CD}_3\text{CHOHCD}_3$) mixture in the C–H stretching region with a molar fraction of 2-propanol at 1, 0.5, 0.4, 0.3, 0.2, 0.1, and 0.05, respectively [Colour figure can be viewed at wileyonlinelibrary.com]

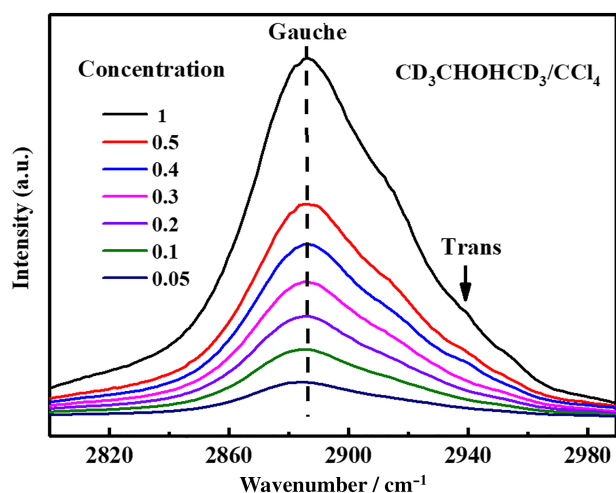


FIGURE 2 Concentration-dependent Raman spectra of deuterated 2-propanol/ CCl_4 mixture in the C-H stretching region with a molar fraction of 2-propanol at 1, 0.5, 0.4, 0.3, 0.2, 0.1, and 0.05, respectively [Colour figure can be viewed at wileyonlinelibrary.com]

solution, the CH stretching band of 2-propanol is almost unchanged in nonpolar CCl_4 solution, indicating that the blue shift in 2-propanol/water mixture should be closely related to H-bonding interactions.

3.2 | Calculated results

To reveal the origin of C-H blue shift observed in 2-propanol/water solution, ab initio quantum chemistry calculations have been performed on a large number of microhydrated clusters containing a 2-propanol monomer with the aim to mimic the hydration process. As a matter of fact, the complicated intermolecular interactions often hinder a clear molecular-level understanding on the effects observed in condensed phase. The information about molecular clusters may provide a route to such a molecular-level interpretation.^[59,60]

2-Propanol molecule has two conformers. Here only gauche conformer was chosen during calculation since the experimental CH stretching spectrum is mainly contributed by gauche conformer. Table 1 summarizes the relative binding energy of the PW_n ($n = 1-6$) clusters corrected by ZPE and BSSE along with the CH stretching wavenumber of methyne group (-CH) of 2-propanol and its blue shift relative to monomer 2-propanol. Also, the geometric parameters involved in the C-H...O H-bond are listed, including C-H bond length, the H-bond distance H...O, and the values of electron density $\rho(r_c)$ and its Laplacian ($\nabla^2\rho(r_c)$) at HBCP. As shown in Figure 3, there are various kinds of H-bonded clusters formed

between 2-propanol and water molecules due to the amphiphilic nature of the alcohol. To be clear, only the low-energy conformers are listed for each kind of n .

As shown in Figure 3, for $n = 1$, only two heterodimers, $\text{PW}_1\text{-a}$ and $\text{PW}_1\text{-b}$, can be formed, in which the OH group of 2-propanol behaves as a proton acceptor and proton donor, respectively. According to the calculations, relative to 2-propanol monomer, the formation of O-H...O hydrogen bond leads to blue shift of CH stretching wavenumber in $\text{PW}_1\text{-a}$ and red shift in $\text{PW}_1\text{-b}$, 22 and -15 cm^{-1} , respectively, which are caused by the intramolecular coupling between vicinal bonds due to the charge transfer from a lone pair of the proton acceptor (O) to the antibonding σ^* orbital of the proton donating bond (O-H),^[61] as shown in Table S1. Therefore, the average C-H wavenumber shift is estimated to be at least 7 cm^{-1} since the calculated $\text{PW}_1\text{-a}$ cluster is more stable than $\text{PW}_1\text{-b}$ with a lower binding energy of 1.21 kcal/mol according to the calculations. This is in agreement with experimental observation that the C-H blue shift occurs upon the addition of water.

When $n = 2$, the most stable cluster is the planar ring structure $\text{PW}_2\text{-a}$, in which all molecules are acting as proton acceptor and proton donor at the same time. It gives a blue shift of 15 cm^{-1} , obviously larger than the averaged 7 cm^{-1} in PW_1 clusters. As shown in Figure 3, the second stable cluster $\text{PW}_2\text{-b}$ is also ring structure with a weak C-H...O H-bond formed, in which the proton donor is the H atom of methyne group of 2-propanol and the proton acceptor is O atom of water. The AIM analysis shows the presence of HBCP at the bond path of C-H...O interaction in $\text{PW}_2\text{-b}$. Also, the calculated parameters on the C-H...O interaction follow within the specified range for the H-bonding interaction, according to International Union of Pure and Applied Chemistry (IUPAC),^[62] such as H...O distance (2.44 Å), the magnitude of the electron density (0.0105), and its Laplace value at the HBCP (0.0355), as shown in Table 1. It can be seen that with the participation of C-H...O H-bond, the C-H blue shift of $\text{PW}_2\text{-b}$ becomes significantly increased to be 65 cm^{-1} . Therefore, both conventional O-H...O and weak C-H...O H-bonds can contribute to C-H blue shift. The former is in an indirect way, whereas the latter is in a direct way.

Similar to $n = 2$, the most stable cluster of $\text{PW}_3\text{-a}$ is planar ring structure, followed by $\text{PW}_3\text{-b}$ with a small energy difference of 0.8 kcal/mol. Both $\text{PW}_3\text{-a}$ and $\text{PW}_3\text{-b}$ clusters give the increased C-H blue shift of 22 and 18 cm^{-1} compared to $\text{PW}_2\text{-a}$, respectively. Different from $\text{PW}_3\text{-a}$, the $\text{PW}_3\text{-b}$ is no longer planar, and it slightly deforms to make a contact with -CH group of 2-propanol, forming a weak C-H...O interaction, as seen from Figure 3. Such change from single-ring to double-ring or folded-ring structures becomes more obvious in the

TABLE 1 Calculated CH stretching wavenumbers (cm^{-1}) and relative binding energies ΔE (in kcal/mol) of 2-propanol-(water) $_n$ clusters (PW $_n$, $n = 1-6$) along the parameters involved in C-H \cdots O interaction

<i>n</i>	Complex	$\nu_{\text{CH}}^{\text{a}}$	$\Delta\nu_{\text{CH}}^{\text{b}}$	$\Delta E_{\text{BSSE+ZPE}}^{\text{c}}$	Parameters of C-H \cdots O interaction				
					R(C-H) ^d	R(H \cdots O) ^e	$\angle\text{CHO}$	$\rho(r)^{\text{f}}$	$\nabla^2\rho(r)^{\text{g}}$
0	propanol	2880	0		1.0986				
1	PW ₁ -a	2902	22	0.00	1.0970				
	PW ₁ -b	2865	-15	1.21	1.0998				
2	PW ₂ -a	2895	15	0.00	1.0972				
	PW ₂ -b	2945	65	2.49	1.0939	2.44	125°	0.0105	0.0355
3	PW ₃ -a	2902	22	0.00	1.0970				
	PW ₃ -b	2898	18	0.81	1.0980	2.75	135°	0.0056	0.0180
	PW ₃ -c	2895	15	3.37	1.0974				
	PW ₃ -d	2941	60	4.33	1.0942	2.50	130°	0.0103	0.0309
4	PW ₄ -a	2889	9	0.00	1.0981				
	PW ₄ -b	2905	25	1.00	1.0965				
	PW ₄ -c	2912	32	1.39	1.0971	2.51	136°	0.0090	0.0293
	PW ₄ -d	2955	75	4.46	1.0931	2.46	126°	0.0092	0.0349
5	PW ₅ -a	2908	28	0.00	1.0975	2.58	130°	0.0078	0.0268
	PW ₅ -b	2904	24	1.36	1.0965				
6	PW ₆ -a	2911	31	0.00	1.0974	2.52	151°	0.0088	0.0276
	PW ₆ -b	2900	20	1.89	1.0969				

^aScaled by a factor of 0.954.

^bThe wavenumber shifts of CH stretching vibration relative to monomer 2-propanol.

^cRelative binding energy corrected by zero-point vibrational energy (ZPE) and basis set superposition error (BSSE) relative to the most stable cluster.

^dThe C-H bond length involved in the C-H \cdots O interaction in the clusters in Å.

^eThe hydrogen-bond distance of C-H \cdots O interaction in the clusters in Å.

^fThe Electron density at hydrogen-bond critical points (HBCP).

^gThe Laplacian of electron density at HBCP.

following PW₃-c and PW₃-d, indicating that with the addition of water molecule the hydrated structure of 2-propanol transitions from two dimension (2D) to three dimension (3D).

When $n = 4$, the most stable cluster, PW₄-a, is still shown to be a planar single-ring structure but its C-H blue shift is only 9 cm^{-1} , decreasing with the increase of water molecules, as seen from Table 1. This is obviously not in agreement with the experimental observation. It should be noted that our theoretical calculations are for isolated gas-phase cluster molecules. Therefore, although the single-ring PW₄-a is the most stable according to the calculations, it is not easy to form a large single ring in the liquid-phase environment with the increase of cluster size due to the influence of surrounding molecules. Even if it can be formed, it will not be stable and may soon be transformed into small folded-ring or double-ring structures like the PW₄-b, whose calculated binding energy is 1.0 kcal/mol higher than PW₄-a. It can be seen that the PW₄-b consists of 3D H-bonding networks stabilized

totally by O-H \cdots O H-bonds, in which C-H blue shift is 25 cm^{-1} , continuing to increase relative to PW₃-a. As seen from Figure 3, the PW₄-c and PW₄-d can be regarded as structural evolution from PW₃-b and PW₃-d with the enhanced C-H \cdots O hydrogen bond, respectively. It can be seen that the H \cdots O distances of C-H \cdots O in PW₄-c is shortened to 2.51 Å relative to 2.75 Å in PW₃-b, while it is shorted to 2.46 Å in PW₄-d relative to 2.50 Å in PW₃-d. This indicates that the C-H \cdots O interaction is enhanced with the hydration process of 2-propanol.

When $n = 5, 6$, the case becomes considerably different from those $n \leq 4$. As shown in Figure 3, there are no single-ring structures in all the calculated clusters, in good agreement with the analysis that a large single-ring cluster is difficult to be stable with the increase of cluster size. Moreover, the most stable clusters, PW₅-a and PW₆-a, are no longer totally connected via O-H \cdots O H-bonds but through a linkage involving both O-H \cdots O and C-H \cdots O interactions. As seen from Table 1, the PW₅-a and PW₆-a give an increased C-H blue shift of 28 and

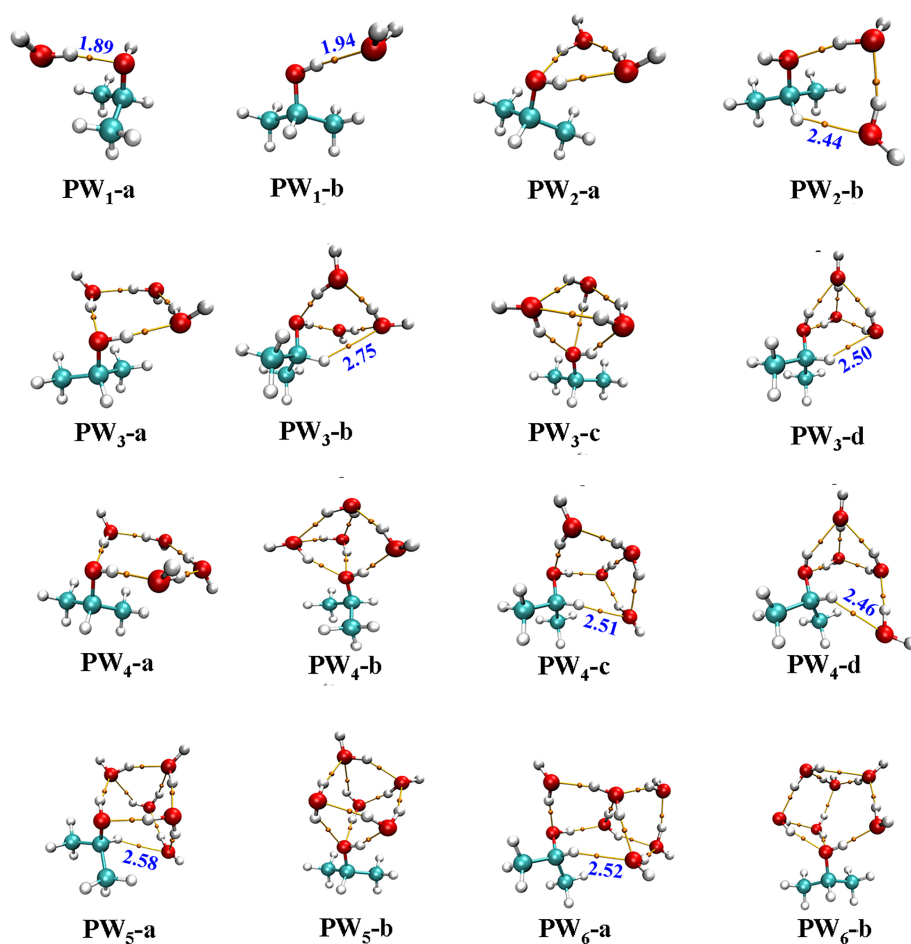


FIGURE 3 Optimized geometric structures of low-energy 2-propanol/water clusters PW_n ($n = 1-6$) calculated at M06-2X/6-311++g(d,p) level. The green atom indicates C atom, red atom indicates O atom, and gray atom indicates H atom. The H-bond critical points (HBCP) from AIM analysis are denoted by golden-yellow dots [Colour figure can be viewed at wileyonlinelibrary.com]

31 cm^{-1} , respectively, whereas the $PW_5\text{-b}$ and $PW_6\text{-b}$ that totally connected by $\text{O-H}\cdots\text{O}$ give a decreased C-H blue shift of 24 and 20 cm^{-1} , respectively. Obviously, the latter is contrary to the experimental observations, indicating that with growing water concentration, the weak $\text{C-H}\cdots\text{O}$ H-bond contributes to cooperative stabilization in the 3D H-bonding networks formed between 2-propanol and water, and this cooperative effect plays a decisive role in further C-H blue shift as water concentration increases. In previous studies, the $\text{C-H}\cdots\text{O}$ H-bond was also found to be playing an important role in providing 3D structure to organic and inorganic supramolecular complexes, molecular recognition, and enzymatic catalysis.^[15,63,64]

From above theoretical analysis, it can be seen that although the DFT calculations cannot fully reproduce condense phase environment in 2-propanol/water mixture, the predicted C-H blue shifts in PW_n clusters is in agreement with experimental results in the overall trend and so provided a qualitative support on the observed C-H blue shift. At relatively high alcohol concentration ($n \leq 4$), the $\text{O-H}\cdots\text{O}$ H-bond plays a dominant role, and with the increase of water concentration, the cooperative effect between $\text{O-H}\cdots\text{O}$ and $\text{C-H}\cdots\text{O}$ H-bonds plays a more significant role and should be responsible for

further increased C-H blue shift. These results not only provide deeper insight into intermolecular interaction of 2-propanol in water solution but also reveal the role of secondary H-bond in hydrated process of amphiphilic molecules containing both polar and nonpolar head groups.

3.3 | Temperature-dependent Raman spectra

It is well known that H-bonding interactions are sensitive to temperature. Generally, the conventional H-bond is destroyed by temperature or pressure. However, in recent studies, it has been demonstrated that weak $\text{C-H}\cdots\text{O}$ H-bond can be enhanced by high temperature or high pressure.^[58,65,66] Since both $\text{O-H}\cdots\text{O}$ and $\text{C-H}\cdots\text{O}$ H-bonds coexist in 2-propanol/water solution, one expects it to show interesting temperature-dependent variations, which can further be used to study the relative importance of intermolecular interactions as the change of external conditions. To this end, the temperature-dependent Raman spectra of deuterated 2-propanol/water solution were measured.

FIGURE 4 Temperature-dependent Raman spectra of deuterated 2-propanol/water mixture at a mole fraction of methanol equal to 0.1 at 5 and 80°C. (a) In the C-H stretching region; (b) in the O-H stretching region [Colour figure can be viewed at wileyonlinelibrary.com]

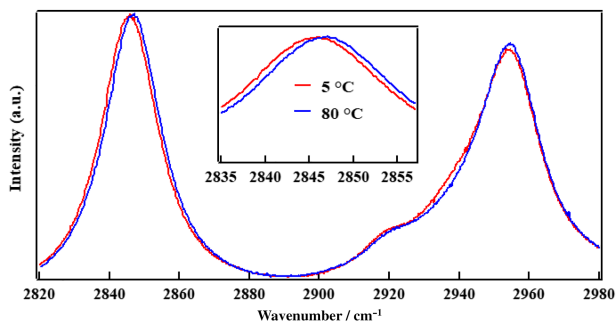
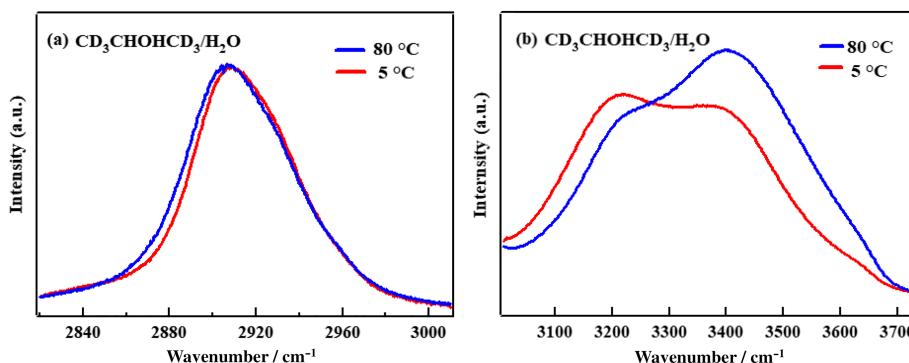


FIGURE 5 Temperature-dependent C-H stretching Raman spectra of methanol/water mixture at a mole fraction of methanol equal to 0.1 at 5°C and 80°C [Colour figure can be viewed at wileyonlinelibrary.com]

Figure 4a presents the temperature-dependent Raman spectra of deuterated 2-propanol/water solution in the C-H stretching region measured at a serial of temperature from 5°C, 25°C, 45°C, 65°C, to 80°C, with a molar fraction of 0.1 concentration. For visual clarity, only the spectra at 5 and 80°C was shown, and the spectra at other temperatures are presented in Figure S1. To be contrasted, the Raman spectra in the O-H stretching region were measured at 5°C and 80°C, as shown in Figure 4b. It can be seen that from 5°C to 80°C, the O-H stretching peak exhibits an obvious blue shift, whereas the C-H stretching peak shows a slight red shift about 2.2 cm⁻¹, which is obtained by the method of center of mass, as listed in Table S2. The blue shift of O-H stretching band results from the destruction of conventional O-H...O H-bond by high temperature, which will lead to red shift of the C-H stretching wavenumber, as shown in Figure 4a. As mentioned above, the previous studies on methanol/water mixture have indicated that the temperature can enhance the C-H...O H-bond, leading to further C-H blue shift at high temperature,^[58] as shown in Figure 5. This behavior is different from C-H red shift observed in the temperature-dependent spectra of 2-propanol/water mixture (Figure 4a). What is the origin of this difference?

TABLE 2 Binding energies (kcal/mol) of hydrated clusters of 2-propanol and methanol calculated at M06-2X/6-311++G(d,p) level

PW _n ^a		MW _n ^b	
Complex	ΔE _{BSSE+ZPE} ^c	Complex	ΔE _{BSSE+ZPE} ^c
PW ₁ -a	-5.25	MW ₁ -a	-4.47
PW ₁ -b	-4.04	MW ₁ -b	-3.98
PW ₂ -a	-14.12	MW ₂ -a	-13.46
PW ₃ -a	-23.82	MW ₃ -a	-22.99

^aPW_n-a denotes the clusters between 2-propanol and water molecules shown in Figure 1.

^bMW_n-a denotes the clusters between methanol and water molecules corresponding to PW_n-a.

^cBinding energy of clusters corrected by zero-point vibrational energy (ZPE) and basis set superposition error (BSSE).

It is known that 2-propanol has two CH₃ groups connecting to carbon atom simultaneously while methanol has only one CH₃ group. As methyl group is an electron-donating group, more methyl groups means more electron density on the O atom of hydroxyl group of 2-propanol, and then facilitate the formation of stronger O-H...O H-bond with the water molecules in solution. This can be confirmed by the calculated binding energy of the hydrated clusters of 2-propanol and methanol, PW_n and MW_n ($n \leq 3$), as summarized in Table 2, where the binding energies of the most stable hydrated clusters of PW_n and MW_n are calculated at the M06-2X/6-311++G(d,p) level. The geometries of MW_n clusters are similar to PW_n-a clusters in Figure 3 by substituting 2-propanol molecule for methanol molecule and not shown here. It can be seen that for each n, the binding energy of PW_n ($n \leq 3$) is larger than that of MW_n, indicating stronger O-H...O H-bonds formed between 2-propanol and water molecules. The stronger the O-H...O H-bond, the greater the C-H red shift due to the destruction of O-H...O H-bond by high temperature. When the C-H red shift from the destruction of O-H...O is larger than the blue shift from the enhancement of C-H...O at high temperature, a slight red-shift occurs, as we

see in Figure 4a. The contrary case is true for methanol-water solution in Figure 5. Therefore, whether it red shifts or blue shifts, the final spectral behavior is a competition and subtle balance of two kinds of H-bonding interactions upon the changes of external conditions such as temperature here.

4 | CONCLUSION

Hydrogen bond, as the most common weak interaction in molecules, plays an important role in related physical, chemical, and biological processes. Conventional H-bonds are ubiquitous in nature, yet the demonstration of weak C-H...O H-bond has proven elusive, especially in water solution, where the conventional H-bonds are usually overwhelming. In this work, we investigated the effect of concentration and temperature on the spectra of deuterated 2-propanol/water mixture (CD₃CHOHCD₃) in the C-H stretching region combined with quantum chemistry calculation. By explaining experimental phenomena that the CH stretching band of 2-propanol blue shifts with the increase of water concentration, we provide a molecular level understanding on what role of the weak C-H...O interaction may play in the hydration process of alcohol. It is shown that with the increase of water concentration, the C-H...O interaction cooperatively stabilizes the three-dimensional H-bonding networks between 2-propanol and water, arousing a continuously increased C-H blue shift. Additionally, the C-H red shift of 2-propanol/water mixture and blue shift of methanol-water mixture at high temperature were interpreted as a result of a competition and subtle balance between C-H...O and O-H...O H-bonding interactions. These results not only provide deeper insight into hydrophobic effect that is the manifestation of the interaction of nonpolar head group with water but also demonstrate that the temperature can be used as a means of triggering and investigating weak C-H...O interaction in liquid.

ACKNOWLEDGEMENT

The present work was supported financially by the National Natural Science Foundation of China (NSFC, 21873002, 21773001, 21727804, 21873089, and 22073088).

ORCID

Yuanqin Yu  <https://orcid.org/0000-0001-7647-8404>

Xiaoguo Zhou  <https://orcid.org/0000-0002-0264-0146>

REFERENCES

- [1] G. A. Jeffrey, W. Saenger, *Hydrogen bonding in biological structures*, Springer-Verlag, Berlin 1990.
- [2] G. R. Desiraju, *The Weak Hydrogen Bond: In Structural Chemistry and Biology*, Oxford University Press, Oxford, New York 1999.
- [3] A. Bhattacharjee, S. Wategaonkar, *J. Phys. Chem. A* **2017**, *121*, 4283.
- [4] S. R. G. Kankanamge, J. B. Ma, R. T. Mackin, F. M. Leonik, C. M. Taylor, I. V. Rubtsov, D. G. Kuroda, *Angew. Chem. Int. Ed.* **2020**, *59*, 17012.
- [5] B. K. Zou, J. D. Xue, Y. Y. Zhao, X. M. Zheng, *Spectrochim. Acta, Part a* **2021**, *255*, 119651.
- [6] A. M. Silski, R. D. Brown, J. P. Petersen, J. M. Coman, D. A. Turner, Z. M. Smith, S. A. Corcelli, J. C. Poutsma, S. A. Kandel, *J. Phys. Chem. C* **2017**, *121*, 21520.
- [7] G. Bulusu, G. R. Desiraju, *J. Indian Inst. Sci.* **2020**, *100*, 31.
- [8] A. Senes, I. Ubarretxena-Belandia, D. M. Engelman, *Proc. Natl. Acad. Sci. U. S. A.* **2001**, *98*, 9056.
- [9] S. Scheiner, *J. Phys. Chem. B* **2009**, *113*, 10421.
- [10] P. Lavanya, S. Ramaiah, A. Anbarasu, *J. Biol. Phys.* **2013**, *39*, 649.
- [11] A. K. Samanta, P. Banerjee, B. Bandyopadhyay, P. Pandey, T. Chakraborty, *J. Phys. Chem. A* **2017**, *121*, 6012.
- [12] S. Ghosh, S. Wategaonkar, *J. Phys. Chem. A* **2019**, *123*, 3851.
- [13] R. C. Johnston, P. H.-Y. Cheong, *Org. Biomol. Chem.* **2013**, *11*, 5057.
- [14] J. H. Aasheim, H. Fliegl, E. Uggerud, T. Bonge-Hansen, O. Eisenstein, *New J. Chem.* **2014**, *38*, 5975.
- [15] L. Jiang, L. Lai, *J. Biol. Chem.* **2002**, *277*, 37732.
- [16] S. K. Singh, M. M. Babu, P. Balaram, *Proteins* **2003**, *51*, 167.
- [17] Y. Gu, T. Kar, S. Scheiner, *J. Am. Chem. Soc.* **1999**, *121*, 9411.
- [18] X. Chang, Y. Zhang, X. Weng, P. Su, W. Wu, Y. Mo, *J. Phys. Chem. A* **2016**, *120*, 2749.
- [19] Y. Z. Mao, M. Head-Gordon, *J. Phys. Chem. Lett.* **2019**, *10*, 3899.
- [20] S. Kawai, T. Nishiuchi, T. Kodama, P. Spijker, R. Pawlak, T. Meier, J. Tracey, T. Kubo, E. Meyer, A. S. Foster, *Sci. Adv.* **2017**, *3*, e1603258.
- [21] H. S. Frank, M. W. Evans, *J. Chem. Phys.* **1945**, *13*, 507.
- [22] R. F. Lama, B. C. Y. Lu, *J. Chem. Eng. Data* **1965**, *10*, 216.
- [23] F. Franks, D. J. G. Ives, *Qual. Rev. Chem. Soc.* **1966**, *20*, 1.
- [24] F. Franks, J. E. Desnoyers, *Water Sci. Rev.* **1985**, *1*, 171.
- [25] F.-M. Pang, C.-E. Seng, T.-T. Teng, M. H. Ibrahim, *J. Mol. Liq.* **2007**, *136*, 71.
- [26] S. Dixit, W. C. K. Poon, J. Crain, *J. Phys. Condens. Matter* **2000**, *12*, L323.
- [27] A.-A. Liu, S. Liu, R. Zhang, Z. Ren, *J. Phys. Chem. C* **2015**, *119*, 23486.
- [28] G.-H. Deng, Y. Shen, H. Chen, Y. Chen, B. Jiang, G. Wu, X. Yang, K. Yuan, J. Zheng, *J. Phys. Chem. Lett.* **2019**, *10*, 7922.
- [29] S. Dixit, J. Crain, W. C. K. Poon, J. L. Finney, A. K. Soper, *Nature* **2002**, *416*, 829.
- [30] S. Dwivedi, J. Mata, S. H. Mushrif, A. L. Chaffee, A. Tanksale, *J. Phys. Chem. Lett.* **2021**, *12*, 480.
- [31] K. Yoshida, S. Ishida, T. Yamaguchi, *Mol. Phys.* **2019**, *117*, 3297.
- [32] C. Corsaro, J. Spooren, C. Branca, N. Leone, M. Broccio, C. Kim, S. H. Chen, H. E. Stanley, F. Mallamace, *J. Phys. Chem. B* **2008**, *112*, 10449.
- [33] J. McGregor, R. Li, J. A. Zeitler, C. D'Agostino, J. H. P. Collins, M. D. Mantle, H. Manyar, J. D. Holbrey, M. Falkowska,

- T. G. A. Youngs, C. Hardacre, E. H. Stitt, L. F. Gladden, *Phys. Chem. Chem. Phys.* **2015**, *17*, 30481.
- [34] J. H. Guo, Y. Luo, A. Augustsson, S. Kashtanov, J. E. Rubensson, D. K. Shuh, H. Agren, J. Nordgren, *Phys. Rev. Lett.* **2003**, *91*, 157401.
- [35] M. Nagasaka, K. Mochizuki, V. Leloup, N. Kosugi, *J. Phys. Chem. B* **2014**, *118*, 4388.
- [36] S. Pothoczki, I. Pethes, L. Pusztai, L. Temleitner, D. Csokas, S. Kohara, K. Ohara, I. Bako, *J. Mol. Liq.* **2021**, *329*, 115592.
- [37] S. Pothoczki, I. Pethes, L. Pusztai, L. Temleitner, K. Ohara, I. Bako, *J. Phys. Chem. B* **2021**, *125*, 6272.
- [38] M. Nagasaka, H. Yuzawa, N. Kosugi, *J. Phys. Chem. B* **2020**, *124*, 1259.
- [39] S. K. Allison, J. P. Fox, R. Hargreaves, S. P. Bates, *Phys. Rev. B* **2005**, *71*, 024201.
- [40] A. K. Soper, L. Dougan, J. Crain, J. L. Finney, *J. Phys. Chem. B* **2006**, *110*, 3472.
- [41] S. Pothoczki, L. Pusztai, I. Bako, *J. Phys. Chem. A* **2019**, *123*, 7599.
- [42] R. K. Lam, J. W. Smith, R. J. Saykally, *J. Chem. Phys.* **2016**, *144*, 191103.
- [43] Y. Q. Yu, Y. X. Wang, K. Lin, N. Y. Hu, X. G. Zhou, S. L. Liu, *J. Phys. Chem. A* **2013**, *117*, 4377.
- [44] Y. Yu, Y. Wang, K. Lin, X. Zhou, S. Liu, J. Sun, *J. Raman Spectrosc.* **2016**, *47*, 1385.
- [45] Y. Q. Yu, Y. X. Wang, N. Y. Hu, K. Lin, X. G. Zhou, S. L. Liu, *Phys. Chem. Chem. Phys.* **2016**, *18*, 10563.
- [46] L. Xing, W. Fan, N. Chen, M. N. Li, X. G. Zhou, S. L. Liu, *J. Raman Spectrosc.* **2019**, *50*, 629.
- [47] R. Kobayashi, J. Normand, K. Raghavachari, A. P. Rendell, J. C. Burant, S. S. Iyengar, J. Tomasi, M. Cossi, J. M. Millam, M. Klene, C. Adamo, R. Cammi, J. W. Ochterski, R. L. Martin, K. Morokuma, O. Farkas, J. B. Foresman, D. J. Fox, Wallingford, CT **2016**.
- [48] L. Tian. <http://www.keinsci.com/research/molclus.html> **2016**.
- [49] Y. Zhao, D. G. Truhlar, *Theor. Chem. Acc.* **2008**, *120*, 215.
- [50] S. F. Boys, F. Bernardi, *Mol. Phys.* **1970**, *19*, 553.
- [51] A. Mandal, M. Prakash, R. M. Kumar, R. Parthasarathi, V. Subramanian, *J. Phys. Chem. A* **2010**, *114*, 2250.
- [52] R. F. W. Bader, *Atoms in Molecules — a Quantum Theory*, Clarendon Press, Oxford, U.K **1990**.
- [53] B. Biswas, S. Mondal, P. C. Singh, *J. Phys. Chem. A* **2017**, *121*, 1250.
- [54] T. Lu, F. Chen, *J. Comput. Chem.* **2012**, *33*, 580.
- [55] Y. Q. Yu, Y. X. Wang, N. Y. Hu, K. Lin, X. G. Zhou, S. L. Liu, *J. Raman Spectrosc.* **2014**, *45*, 259.
- [56] V. Sharma, S. Schluecker, S. K. Srivastava, *J. Raman Spectrosc.* **2021**, *52*, 1722.
- [57] B. Yang, Z. Liu, S. Wang, C. Sun, Z. Men, *J. Raman Spectrosc.* **2021**, *52*, 1440.
- [58] Y. Yu, W. Fan, Y. Wang, X. Zhou, J. Sun, S. Liu, *J. Phys. Chem. B* **2017**, *121*, 8179.
- [59] G. Matisz, A. M. Kelterer, W. M. F. Fabian, S. Kunsagi-Mate, *Phys. Chem. Chem. Phys.* **2015**, *17*, 8467.
- [60] S. G. Zetterholm, G. A. Verville, L. Boutwell, C. Boland, J. C. Prather, J. Bethea, J. Cauley, K. E. Warren, S. A. Smith, D. H. Magers, N. I. Hammer, *J. Phys. Chem. B* **2018**, *122*, 8805.
- [61] A. Karpfen, *Phys. Chem. Chem. Phys.* **2011**, *13*, 14194.
- [62] E. Arunan, G. R. Desiraju, R. A. Klein, J. Sadlej, S. Scheiner, I. Alkorta, D. C. Clary, R. H. Crabtree, J. J. Dannenberg, P. Hobza, H. G. Kjaergaard, A. C. Legon, B. Mennucci, D. J. Nesbitt, *Pure Appl. Chem.* **2011**, *83*, 1619.
- [63] J. T. Makuvaza, D. L. Kokkin, J. L. Loman, S. A. Reid, *J. Phys. Chem. A* **2019**, *123*, 2874.
- [64] P. Banerjee, P. Pandey, B. Bandyopadhyay, *Spectrochim. Acta, Part a* **2021**, *253*, 119550.
- [65] H. C. Chang, J. C. Jiang, C. C. Su, L. C. Lu, C. J. Hsiao, C. W. Chuang, S. H. Lin, *J. Phys. Chem. A* **2004**, *108*, 11001.
- [66] F. Meersman, J. Wang, Y. Q. Wu, K. Heremans, *Macromolecules* **2005**, *38*, 8923.

SUPPORTING INFORMATION

Additional supporting information can be found online in the Supporting Information section at the end of this article.

How to cite this article: T. Li, W. Fan, J. Sun, Y. Yu, X. Zhou, C. Xie, S. Liu, *J Raman Spectrosc* **2022**, *53*(9), 1551. <https://doi.org/10.1002/jrs.6413>